

TIPP 2011 – Technology and Instrumentation in Particle Physics 2011

## Development and Characterization of CdZnTe Detectors for Neutrino Physics Research

T. Kutter<sup>a,\*</sup>, J. Miyamoto<sup>a</sup>

<sup>a</sup>Department of Physics & Astronomy, Louisiana State University, 202 Nicholson Hall, Baton Rouge, LA 70803, USA

---

### Abstract

CdZnTe crystals contain 9 double beta decay isotopes and can serve simultaneously as source and detector in a search for neutrino-less double beta decay. In particular,  $^{116}\text{Cd}$  and  $^{130}\text{Te}$  are suitable isotopes in such a search due to their high Q-values. The endpoint of the beta spectra resulting from double-beta decay of these isotopes is well above natural gamma lines which constitute backgrounds to a potential signal. Detectors for neutrino-less double beta decay searches require good energy resolution and effective background rejection. Both properties can be realized with position sensitive pixilated detectors that have particle tracking capabilities. CdZnTe detectors are promising detectors to satisfy these criteria and have the additional advantage of room temperature operation. We are developing and characterizing the performance of co-planar and pixilated CdZnTe detectors, study their charged particle tracking capabilities and evaluate their use in future neutrino-less double beta decay search experiments. Results from our laboratory measurements will be presented.

© 2012 Published by Elsevier B.V. Selection and/or peer review under responsibility of the organizing committee for TIPP 11. Open access under [CC BY-NC-ND license](https://creativecommons.org/licenses/by-nc-nd/4.0/).

*Keywords:* CZT; detector development; neutrino; neutrinoless double beta decay

---

### 1. Introduction

In recent years neutrino physics has made tremendous progress in understanding the properties of neutrinos [1-5]. While a clearer picture of neutrino properties is starting to emerge numerous questions addressing neutrino mass and the nature of neutrinos (e.g. Dirac versus Majorana) remain to be explored. Searches for neutrinoless double beta decay may provide new insights if such rare events are observed. The discovery of neutrino oscillations [1-5] has spurred renewed interest in double beta decay searches as

\* Email: [kutter@phys.lsu.edu](mailto:kutter@phys.lsu.edu)

the next generation of experiments may have sufficient sensitivity to see a signal if an inverted neutrino mass hierarchy is realized in nature.

A multitude of candidate double beta decay isotopes exists and has been studied in experiments over the past decades [6]. Amongst the candidate isotopes the most preferable ones have high Q values in order for the signal search region to be above the energy of naturally occurring gamma lines from radioactivity in the detector and surrounding materials. Experimental setups in which the detector also serves as source are preferable so as to increase the detection efficiency and ultimately the sensitivity of the experiment. In addition, detectors are required to have excellent energy resolution in order to be able to separate potential signal from backgrounds.

The increased demand and commercialization of CdZnTe crystal production has led to high quality CdZnTe detectors which have exhibited good energy resolution. CdZnTe material contains 9 double beta decay candidate isotopes of which  $^{116}\text{Cd}$ ,  $^{106}\text{Cd}$  and  $^{130}\text{Te}$  are the most promising ones for a search for neutrinoless double beta decay due to their high Q-values of 2.81 MeV, 2.77 MeV and 2.53 MeV, respectively. The use of CdZnTe allows the simultaneous study of several isotopes at once. While the energy resolution in Ge detectors is better still, CdZnTe detectors can be operated at room temperature which is an advantage for a long term experiment. The use of CdZnTe crystals allows for a modular design and avoids problematic issues related to scaling of the setup to a very large mass to reach an ultimate sensitivity. The natural abundances of  $^{116}\text{Cd}$ ,  $^{106}\text{Cd}$  and  $^{130}\text{Te}$  are 7.5%, 1.2% and 33.8%, respectively. Hence, an enrichment of the relevant isotopes in the crystal production is not absolutely required but it would be desirable to further increase the sensitivity of an experiment employing CdZnTe detectors in a search for neutrinoless double beta decay.

The present paper describes our investigation of the properties of CdZnTe crystals with different readout configurations. First we describe the measured performance of detectors with co-planar grid electrodes to establish a baseline. Next we study the characteristics of a detector with a pixilated electrode pattern. The purpose of a pixilated electrode design is three-fold: Improvements in energy resolution, the possibility to identify multi-hit events and ultimately, if pixel sizes can be reduced sufficiently, to perform particle tracking in 3 dimensions are the main reasons to investigate pixilated CdZnTe detectors. All of these potential improvements would lead to better background rejection and hence better sensitivity in a search for neutrinoless double beta decay.

## 2. Detector Description and Performance

The performance and operating characteristics of a co-planar and a pixilated  $\text{Cd}_{0.9}\text{Zn}_{0.1}\text{Te}_{1.0}$  detector have been studied. Both detector crystals were manufactured by eV-products/Endicott [7] and included the metallization and electrode patterning. The outer crystal dimensions of the co-planar and pixilated detectors are  $10\times 10\times 10\text{mm}^3$  and  $11\times 11\times 5\text{mm}^3$ , respectively. The co-planar detector crystal weighs about 5.9 g and features clear passivation coating while the pixilated detector has a red passivation coating which is known to contain relatively more radio impurities [8].

### 2.1. Coplanar CdZnTe Detector

The concept used in co-planar detectors is based on an idea which was first realized, proposed and implemented for gas ionization chambers by Luke [9]. The key issue is that electrons and ions have different drift speeds which differ by few orders of magnitude. Hence, in large volume detectors the combined induced charge by electrons and ions depends on the location of the ionization and can vary greatly. Variations in the induced charge lead to worse energy resolution which is of course an undesirable effect. By installing a Frisch grid close to the anode (see figure 1), the charge induction due to

ions is strongly suppressed and the device effectively becomes a single carrier detector. In case of CdZnTe crystals the charge carriers are electrons and holes which also have greatly differing mobility. The hole contribution to the signal can be removed by alternating collecting and non-collecting electrodes which are biased at different potentials. Figure 1 shows a conceptual design of a Frisch grid and a coplanar electrode pattern. Electrons and holes drift in opposite directions and once electrons come in proximity of the anode, they are preferentially collected by the positively biased electrode. The induced current due to charges moving in the vicinity of an electrode is given by the Shockley-Ramo theorem [10,11] and is different for the two co-planar electrodes.

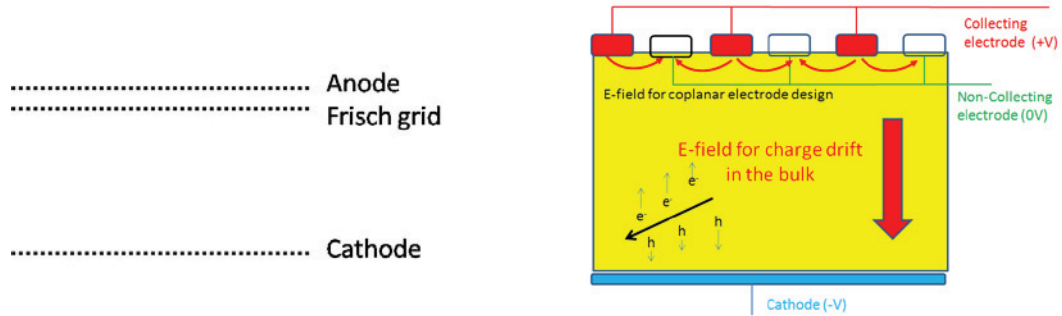


Fig. 1. Conceptual layout of a Frisch grid detector (a) and a detector featuring a co-planar electrodes (b).

The collecting and non-collecting electrodes are connected to a charge sensitive pre-amplifier each, the signal of on the non-collecting electrode is inverted at the analog stage before both are added together and fed into a shaper and Multi Channel Analyzer (MCA). Effectively, the two signals from the co-planar electrodes are subtracted to remove the signal contribution from the holes and to increase the signal amplitude.

In our test setup we used Cremat CR-110 preamplifiers, standard NIM modules for signal inversion and a CAEN N625 quad linear FIFO for signal addition before shaping the signal with an ORTEC 570 shaping amplifier (shaping time set to  $2\mu\text{s}$ ) and recording it with an AMPTEK 8000A pocket MCA. Our setup permitted to obtain a copy of the pre-amplified signals from the collecting and non-collecting grids as well as the combined signal by means of the FIFO and record each of these signals with a Tektronix MSO 5204 mixed signal digital Oscilloscope (2GHz;10GS/s) which recorded the signal transients. The coplanar grid has  $200\mu\text{m}$  wide electrodes which are interspersed with  $300\mu\text{m}$  wide gaps. The anode side is surrounded by a guard ring which leaves a  $250\mu\text{m}$  wide space to all four edges and reduces the active detector area by  $600\mu\text{m}$  on all four sides. The cathode consists of a continuous Au based electrode. The electrode patterning prior to contacting can be seen in Figure 2. Electrical contacts to the two anode grids and the guard ring as well as the cathode side were established using conductive epoxy.

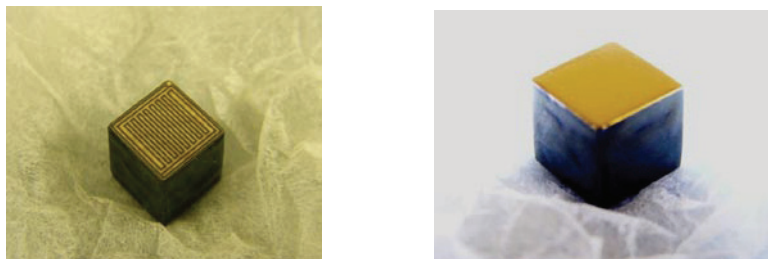


Fig. 2. Anode (a) and cathode (b) side of our  $10\times 10\times 10\text{ mm}^3$  co-planar CdZnTe detector.

The quality of the contacts was studied by means of repeated temperature dependent noise measurements and was found to be good. A finely collimated  $^{137}\text{Cs}$  source was used to illuminate the detector at various depths and the signal transients were studied. Figure 3 shows the signal transients for the collecting and the non-collecting electrodes as well as the combined signal for three different interaction depths.

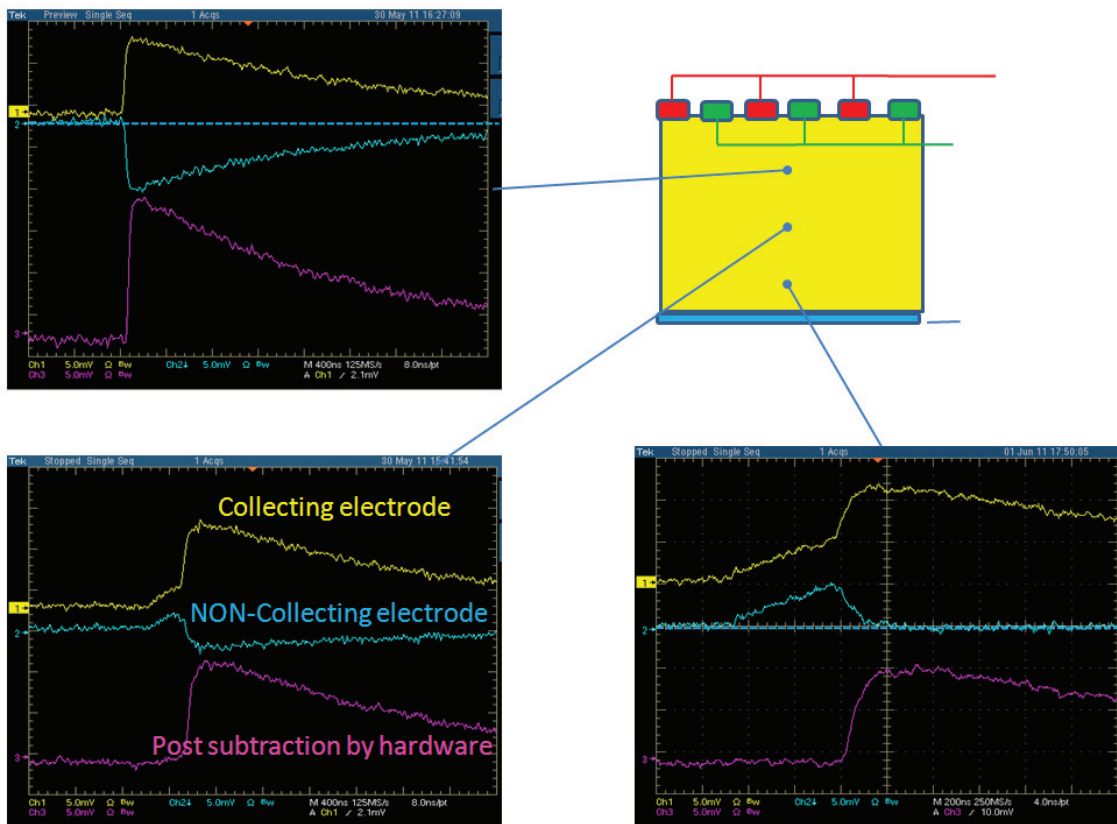


Fig. 3. Signal transients from the collecting, non-collecting co-planar grids and the combined signal as function of depth of interaction in the  $10 \times 10 \times 10 \text{ mm}^3$  CdZnTe crystal.

For particle interactions near the anode the amplitude of the signal on the non-collecting electrode is purely negative while for interactions near the cathode it is purely positive. Interactions in the bulk of the crystal the signal of the non-collecting electrode is bi-polar. A fast fall-off seen in the signal shape of the non-collecting electrode is due to electrons drifting away from the non-collecting electrode. The amplitude of this signal decreases with increased distance to the anode. The earlier and slowly rising part of the signal on the non-collecting electrode seen for interactions in the bulk and near the cathode is caused by induced charge by electrons and holes drifting in the bulk crystal. A similar slow rise is seen in the transient of the collecting electrode. In the collecting electrode the slowly rising signal is superimposed with a later fast rise which is due to fast moving electrons in the vicinity of the co-planar electric field. Hence, a subtraction of the signal on the non-collecting electrode from the signal on the collecting electrode will remove the signal component caused by the holes and electrons drifting in the bulk of the crystal. At the same time, the amplitude of the signal induced by electrons drifting in the co-planar electric field increases for events originating in the bulk of the crystal. Measurements with our co-

planar detector setup confirm this well known and well studied ability of co-planar detectors to correct the amplitude loss due to hole trapping.

In our setup the cathode was biased at 2000V and a dedicated measurement was carried out in order to optimize the co-planar voltage. Figure 4 shows the recorded energy spectra in response to a  $^{137}\text{Cs}$  source for six different co-planar voltages in the range from 0 to 100V.

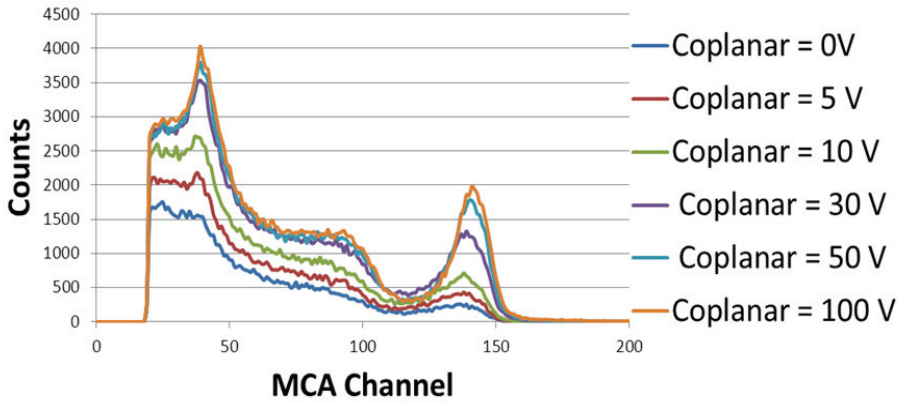


Fig. 4. Energy spectra recorded by a  $10\times 10\times 10\text{mm}^3$  co-planar CdZnTe detector in response to a  $^{137}\text{Cs}$  source and for six different values of the co-planar voltage.

The 662 keV gamma peak is clearly visible for co-planar voltages above 30V while increases above 50V only lead to minor improvements. Because of the relatively small gap between collecting and non-collecting electrodes of  $300\mu\text{m}$  even a small voltage of 30V is sufficient to make the co-planar field effective. In our setup we typically chose a co-planar voltage of 60V.

The energy response of the co-planar detector has been studied with a variety of gamma sources in the energy range from 276 keV to 1.62 MeV. Table 1 summarizes the source isotopes, the pertinent gamma energies and the measured relative FWHM energy resolutions. Even after 120 hours of data taking with the  $^{228}\text{Th}$  source a meaningful energy resolution measurement at the 2.6 MeV gamma line was not possible due to limited statistics resulting directly from the relatively high energy and small detector size.

Source isotope	$E_\gamma$ [keV]	$\Delta E_{\text{FWHM}}/E$ [%]
$^{133}\text{Ba}$	276, 302	12.97
	355, 383	7.02
$^{137}\text{Cs}$	662	7.0
$^{22}\text{Na}$	511	8.8
	1274	5.9
$^{60}\text{Co}$	1173.2	3.95
	1332.5	3.89
$^{228}\text{Th}$	1621	2.68

Table 1. Measured energy resolutions with a  $10\times 10\times 10\text{mm}^3$  co-planar CdZnTe detector in response to a variety of gamma sources.

The measured energy resolutions are representative of the detector setup and include electronics noise inherent to the detector setup. The electronics noise was measured separately at room temperature with a pulse generator signal and a shaping time of 2  $\mu$ s. The width of the electronics noise was found to be constant as function of injected charge. Figure 5 shows the relative energy resolution in percent (FWHM/centroid) as function of the input charge. The input charge was converted to an energy equivalent and is at the sub percent level above equivalent energies of 2 MeV.

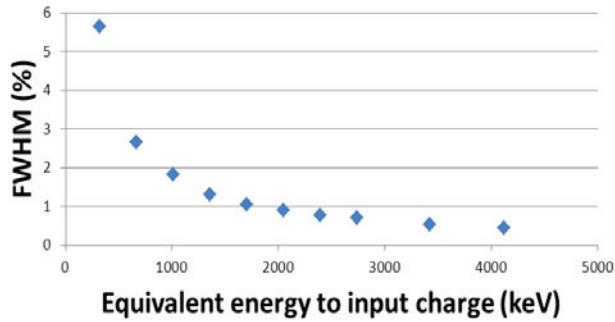


Fig. 5. Contribution of inherent electronics noise to the energy resolution of the detector setup as measured with a pulse generator and a shaping time of 2 $\mu$ s at room temperature.

We studied the linearity of the detector response and found it to be linear in the energy range covered by the sources listed in table 1. Figure 6 shows the MCA centroid of each of the energy resolution measurements as function of energy. The error bars are the FWHM energy resolutions listed in table 1.

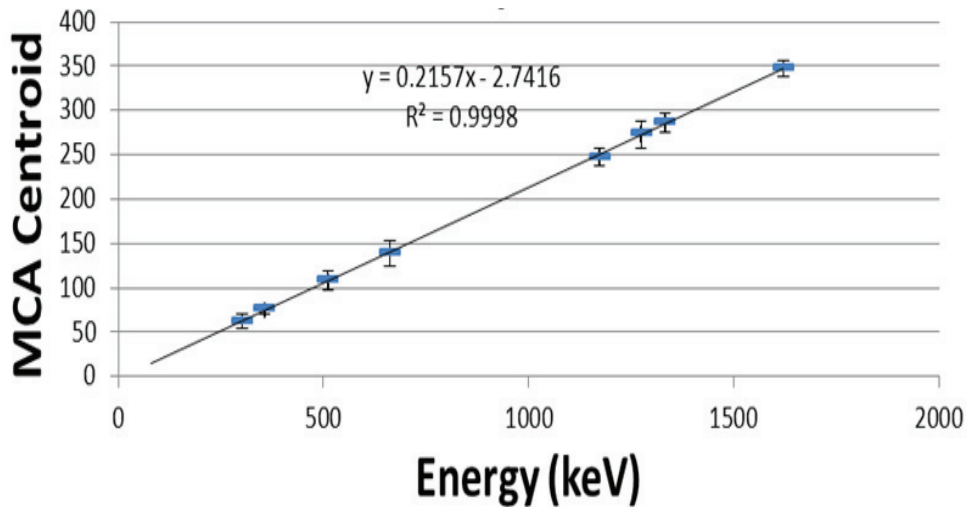


Fig. 6. Shown is the MCA centroid as function of energy for source measurements at various energies for the 10 $\times$ 10 $\times$ 10mm<sup>3</sup> co-planar CdZnTe detector. The error bars are the FWHM energy resolutions of the detector at the specified energies.

In addition, we investigated the dynamic range of the detector with  $^{90}\text{Sr}$  and  $^{106}\text{Ru}$  beta sources. The detector spectrum in response to the latter is shown in figure 7. While the spectral shape agrees with expectation a detailed measurement of the spectral endpoint would require better statistics.

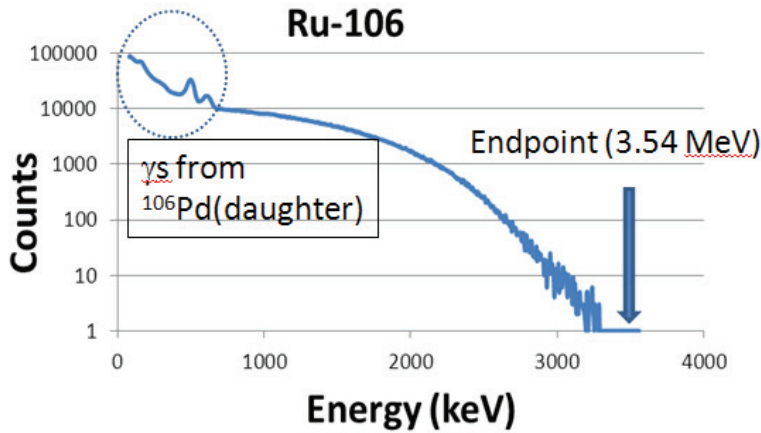


Fig. 7. Energy spectrum of the  $10\times 10\times 10\text{mm}^3$  co-planar CdZnTe detector in response to a  $^{106}\text{Ru}$  beta source.

## 2.2. Pixilated CdZnTe Detector

The segmented detector used in our studies consists of  $4\times 4$  pixels with a pixel size of  $2.0\times 2.0\text{mm}^2$ , a pixel pitch of 2.1 mm and centered on the detector. The pixels are surrounded by a 1 mm wide guard ring which is  $250\mu\text{m}$  away from each of the four crystal edges. The pixels were connected to a 16 channel testing platform (MultiPIX) from eV-products/Endicott International which contains a 16 channel preamplifier and shaper ASIC. The 16 shaped signals were recorded with a set of four Tektronix oscilloscopes or alternatively, a single channel was recorded with an AMPTEK 8000A pocket MCA. While a more detailed account of our studies using this 16 pixel detector is given in [12], here we compare the energy resolutions of the pixel detector with the co-planar detector setup using the  $^{60}\text{Co}$  source. Figure 8 shows the  $^{60}\text{Co}$  energy spectra as recorded by both detectors. At energies of 1.3 MeV the FWHM energy resolution was measured to be 3.89% for the co-planar detector and 1.5% for the pixel detector. The measurement for the pixel detector represents an average over all 16 pixels. Two effects contribute to the superior energy resolution of the pixel detector, namely the “small pixel” effect [13,14] and the reduced charge trapping effect in the pixel detector due to its smaller height.

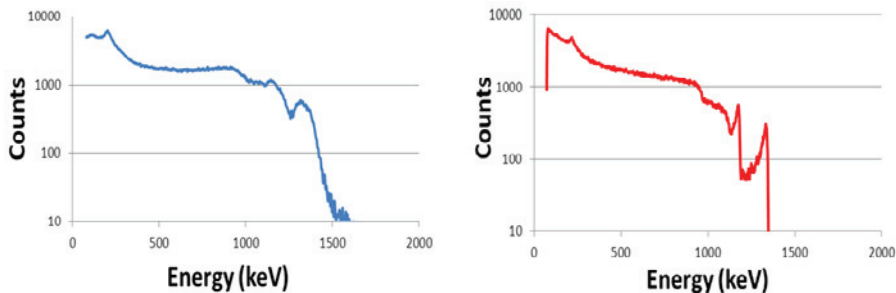


Fig. 8. Energy spectra for a  $^{60}\text{Co}$  source recorded with the co-planar (a) and the pixel (b) detector.



### 2.3. Summary and Discussion

After optimizing the operating voltages for a  $10 \times 10 \times 10 \text{ mm}^3$  co-planar CdZnTe detector we performed a study of co-planar CdZnTe detector signals from the collecting and non-collecting anode as function of depth of interaction in the crystal. We observed a distinct dependence of signal shape on the depth of interaction. In future measurements we aim to exploit the signal shape to determine the depth of interaction on an event by event basis. We also studied the energy resolution, linearity and dynamic range of the detector setup over a wide range of gamma and beta energies. Currently work is in progress to measure the dependence of the energy resolution on the depth of interaction. The energy resolutions of the co-planar and a pixel detector were compared and we observed the pixel detector to have superior energy resolution. Further investigation is required to quantize the magnitude of improvement due to the pixel configuration because in our setup the two detectors had different thickness.

### Acknowledgements

The authors would like to thank the Board of Regents of the State of Louisiana who supported this work under grant no. LEQSF (2008-11)-RD-A-08.

### References

- [1] SNO Collaboration, S.N. Ahmed et al., *Phys. Rev. Lett.* **87** (2001) 071301; S.N. Ahmed et al., *Phys. Rev. Lett.* **89** (2002) 011301; S.N. Ahmed et al., *Phys. Rev. Lett.* **92** (2004) 181301; B. Aharmim et al., *Phys. Rev. C* **72** (2005) 055502
- [2] Super Kamiokande Collaboration, Y. Fukuda et al., *Phys. Rev. Lett.* **81** (1998) 1562
- [3] K2K Collaboration, E. Aliu et al., *Phys. Rev. Lett.* **94** (2005) 081802; M.H. Ahn et al., *Phys. Rev. D* **74** (2006) 072003
- [4] MINOS Collaboration, P. Adamson et al., *Phys. Rev. Lett.* **101** (2008) 131802; P. Adamson et al., *Phys. Rev. Lett.* **103** (2009) 261802;
- [5] KamLAND Collaboration, K. Eguchi et al., *Phys. Rev. Lett.* **92** (2004) 071301; T. Araki et al., *Phys. Rev. Lett.* **94** (2005) 081801
- [6] S.R. Elliott, P. Vogel, *Annu. Rev. Nucl. Part. Sci.* **52** (2002) 115-51; doi:10.1146/annurev.nucl.52.050102.090641
- [7] <http://www.evmicroelectronics.com/>
- [8] T. Bloxham et al., *Phys. Rev. C* **76** (2007) 025501
- [9] P.N. Luke, *Appl. Phys. Lett.* **65** (1994) 2884
- [10] W. Shockley, *Journal of Applied Physics* **9** (1938) 10: 635. doi:10.1063/1.1710367
- [11] S. Ramo, *Proceedings of the IRE* **27** (1939) 9: 584–585. doi:10.1109/JRPROC.1939.228757
- [12] J. Miyamoto, T. Kutter et al., *Proceedings of the IEEE* **2010**, R05-46
- [13] H.H. Barrett, J.D. Eskin and H.B. Barber, *Phys. Rev. Lett.* **75**, 156 (1995)
- [14] J.D. Eskin, H.H. Barrett and H.B. Barber, *J. Appl. Phys.* **85**, 647 (1999)